NPS-53Zh75102

NAVAL POSTGRADUATE SCHOOL

Monterey, California

A NUMERICAL MODEL FOR THE EFFECT OF OCEAN WAVES ON THE ADJACENT AIRFLOW

A.L. Schoenstadt R.T. Williams

K.L. Davidson B.C. Stauffer

K.G. Dunning

October 1975

Approved for public release; distribution unlimited

Prepared for:
Chief of Naval Research, Arlington, Virginia 22217

NAVAL POSTGRADUATE SCHOOL
Monterey, California

Rear Admiral Isham Linder
Superintendent

Jack R. Borsting
Provost

The work reported herein was supported in part by the Foundation Research Program of the Naval Postgraduate School with funds provided by the Chief of Naval Research, and in part by the Ocean Science Division of the Office of Naval Research.

This report was prepared by:

UNCLASSIFIED

SECURITY CLASSIFICATION OF THIS PAGE (When Data Entered)

REPORT DOCUMENTATION PAGE		READ INSTRUCTIONS BEFORE COMPLETING FORM
1. REPORT NUMBER NPS-53Zh75102	2. GOVT ACCESSION NO.	3. RECIPIENT'S CATALOG NUMBER
4. TITLE (and Subtitle) A NUMERICAL MODEL FOR THE EFFECT OF OCEAN WAVES ON THE ADJACENT AIRFLOW		5. TYPE OF REPORT & PERIOD COVERED Final 6. PERFORMING ORG. REPORT NUMBER
7. AUTHOR(s) A.L. Schoenstadt, R.T. Williams, K.L. Davidson, B.C. Stauffer, K.G. Dunning		8. CONTRACT OR GRANT NUMBER(s)
9. PERFORMING ORGANIZATION NAME AND ADDRESS Naval Postgraduate School Monterey, California 93940		10. PROGRAM ELEMENT, PROJECT, TASK AREA & WORK UNIT NUMBERS 6358N ;Task-18726 N0002475WR52221
11. CONTROLLING OFFICE NAME AND ADDRESS Chief of Naval Research, Arlington, VA 22217		12. REPORT DATE October 1975 13. NUMBER OF PAGES 31
14. MONITORING AGENCY NAME & ADDRESS(if different from Controlling Office)		15. SECURITY CLASS. (of this report) UNCLASSIFIED 15a. DECLASSIFICATION/DOWNGRADING SCHEDULE

16. DISTRIBUTION STATEMENT (of this Report)

Approved for public release; distribution unlimited.

17. DISTRIBUTION STATEMENT (of the abstract entered in Block 20, if different from Report)

18. SUPPLEMENTARY NOTES

19. KEY WORDS (Continue on reverse side if necessary and identify by block number)

Wave-Wind Interaction
Eddy Viscosity
Turbulence
Numerical Modeling

20. ABSTRACT (Continue on reverse side if necessary and identify by block number)

The inclusion of non-linear terms in a model for the effect of a fully developed wave field on the overlying airflow is investigated by numerical techniques. The model incorporates turbulence effects by use of an eddy viscosity term. The non-linear terms are shown to cause significant deviations from the linear results. Both linear and non-linear results are compared with observational studies, and significant discrepancies noted.

DD FORM 1 JAN 73 1473 EDITION OF 1 NOV 65 IS OBSOLETE
S/N 0102-014-6601 |

UNCLASSIFIED

SECURITY CLASSIFICATION OF THIS PAGE (When Data Entered)

SUMMARY

In 1970, Yefimov proposed a linearized model for predicting the effect of water waves on the adjacent wind flow. We investigate the impact of the non-linear terms neglected in his model. In this investigation, the sea surface is described by a single harmonic in x and the wave induced motion in the atmosphere is restricted to this harmonic. Buoyancy effects are neglected and the turbulent fluxes of momentum are approximated in terms of an eddy viscosity. The equations are integrated numerically until a steady-state is achieved. These solutions show that the nonlinear terms which were neglected by Yefimov are important, and that they generally lead to a smaller response. The numerical solutions for the mean wind are compared with observations obtained by Davidson and Brutsaert. Although the numerical solutions show some local agreement with the observations, the general behavior is at variance with the observations.

TABLE OF CONTENTS

LIST OF FIGURES

1. Introduction

In this paper a numerical model is formulated to predict the effect of water waves on the adjacent air flow. Data described by Davidson (1974) and Brutsaert (1973) show the effect of water waves on the mean wind. Many studies of the air flow over waves have been carried out for the purpose of determining wave growth [Miles (1957), Phillips (1957), Davis (1970, 1972), Lee (1972)]. Reynolds and Hussain (1972) and Davis (1970, 1972), and Yefimov (1970) emphasized the importance of including the wave-related turbulent Reynolds stresses; these stresses were neglected in the linear model by Miles (1957). We will follow the formulation of Yefimov (1970) except that we will solve the initial value problem rather than the steady state equations. This is because we wish to include the nonlinear interaction between the wave induced motions and the mean flow. We shall see that these interactions are important.

This study treats a single harmonic, fully developed (not affected by the air motion), water wave field. The wave induced motion in the atmosphere is also restricted to one harmonic in x, but the amplitude and phase of the harmonic are free to vary. Actually as shown by Lee (1972), nonlinear effects produce higher harmonics. We neglect these effects because we are mainly concerned with the more easily observed effects on the mean wind. The equations for a homogeneous fluid are written in terms of the Fourier coefficients of the wave, finite differences introduced, and the equations integrated until a steady state is reached. These integrations are carried out for a number of different cases and the results are compared with the observations of Davidson (1974). In order to obtain better agreement with the observations, other boundary conditions and other diffusion coefficients are suggested. The nonlinear effects on the mean wind are investigated by comparison with the linear solutions.

Observational results used in comparisons were obtained from eddy correlation measurements of the momentum flux along with measurements of the mean wind at several levels and wave height measurements. The results were interpreted (Davidson, 1974) with respect to the dependence of the drag coefficient on the non-dimensional parameter, c/U_* , where c corresponds to the phase speed at the swell frequency and U_* is the friction velocity, $U_* = (\tau/c)^{1/2}$. This dependence of the drag coefficient on the wave influence was extended in order to estimate the wave influence on the mean wind profile. The latter is what we examine in this study.

2. Basic equations

The equations for a homogeneous fluid are

$$\frac{\partial \underset{\sim}{V}}{\partial t} + \underset{\sim}{V} \cdot \nabla \underset{\sim}{V} = - \nabla p + \underset{\sim}{F} , \tag{1}$$

$$\nabla \cdot \underset{\sim}{V} = 0 , \tag{2}$$

where

$$F_x = \frac{\partial}{\partial x} (- \overline{u'^2}) + \frac{\partial}{\partial z} (- \overline{u'w'}) , \tag{3}$$

$$F_z = \frac{\partial}{\partial x} (- \overline{u'w'}) + \frac{\partial}{\partial z} (- \overline{w'^2}) . \tag{4}$$

In this formulation, the turbulent Reynolds stresses are assumed to be independent of y and p is the non-hydrostatic pressure divided by the density. The overbars represent local time averages, and u' and w' are the turbulent velocity fluctuations. The portion of the velocity field which is averaged over the turbulence time scale is given by

$$\underset{\sim}{V} = [U(z,t) + u(x,z,t)] \, \underset{\sim}{i} + w(x,z,t) \, \underset{\sim}{j} , \tag{5}$$

where U is the spatially averaged (mean) wind, and u and w are departures. Thus

$$\tilde{u} = \tilde{w} = 0 ,$$

where $(\tilde{\ })$ is the average over one wavelength in x.

We shall follow Yefimov (1970) in representing the turbulent fluxes by

$$-\overline{u'w'} = \tau = K\frac{\partial U}{\partial z} + \nu\left(\frac{\partial u}{\partial z} + \frac{\partial w}{\partial x}\right) , \tag{6}$$

$$\overline{u'^2} = \overline{w'^2} . \tag{7}$$

Note that a mathematical treatment given later by Davis (1974) tends to justify the eddy viscosity form (6).

If (5), (6) and (7) are now substituted into (1), (3) and (4), and the curl $(\underset{\sim}{j} \cdot \underline{\nabla}x)$ of (1) is then taken, the following equation for the vorticity $(\xi = \frac{\partial u}{\partial z} - \frac{\partial w}{\partial x})$ arises:

$$\frac{\partial \xi}{\partial t} + U\frac{\partial \xi}{\partial x} + w\frac{\partial^2 U}{\partial z^2} + u\frac{\partial \xi}{\partial x} + w\frac{\partial \xi}{\partial z} = \frac{\partial^2}{\partial z^2}\left[K\frac{\partial U}{\partial z} + \nu\left(\frac{\partial u}{\partial z} + \frac{\partial w}{\partial x}\right)\right] - \nu\left(\frac{\partial^3 u}{\partial x^2 \partial z} + \frac{\partial^3 w}{\partial x^3}\right) . \tag{8}$$

(Note in this derivation, $\partial U/\partial t$ has been neglected, and the continuity equation (2) has also been used.)

Equation (8) can further be separated into spatially stationary and non-stationary parts by averaging over one wavelength, then subtracting the averaged equation and neglecting the non-stationary perturbation products. This yields, for the stationary part

$$\widetilde{u\frac{\partial \xi}{\partial x}} + \widetilde{w\frac{\partial \xi}{\partial z}} = \frac{\partial^2}{\partial z^2}\left(K\frac{\partial U}{\partial z}\right) . \tag{9}$$

and, for the non-stationary:

$$\frac{\partial \xi}{\partial t} + U\frac{\partial \xi}{\partial x} + w\frac{\partial^2 U}{\partial z^2} = \frac{\partial^2}{\partial z^2}\left[\nu\left(\frac{\partial u}{\partial z} + \frac{\partial w}{\partial x}\right)\right] - \nu\left[\frac{\partial^3 u}{\partial x^2 \partial z} + \frac{\partial^3 w}{\partial x^3}\right] . \tag{10}$$

Since the motion is non-divergent (2), a stream function can be defined such that

$$u = \frac{\partial \psi}{\partial z} , \quad w = - \frac{\partial \psi}{\partial x} . \tag{11}$$

When these relations are introduced into (10), it becomes

$$\left(\frac{\partial}{\partial t} + U\frac{\partial}{\partial x}\right)\left(\frac{\partial^2 \psi}{\partial x^2} + \frac{\partial^2 \psi}{\partial z^2}\right) - \frac{\partial \psi}{\partial x}\frac{\partial^2 U}{\partial z^2} = \frac{\partial^2}{\partial z^2}\left[\nu\left(\frac{\partial^2 \psi}{\partial z^2} - \frac{\partial^2 \psi}{\partial x^2}\right)\right] - \nu\left[\frac{\partial^4 \psi}{\partial x^2 \partial z^2} - \frac{\partial^4 \psi}{\partial x^4}\right] . \tag{12}$$

Now we introduce sinusoidal variations and look for solutions which move with the speed c of the water waves

$$\psi = A(z,t) \cos [k(x-ct)] + B(z,t) \sin [k(x-ct)] . \tag{13}$$

Substitute (13) into (12) and separate the sine and cosine terms. Equating the coefficients of the cosine terms gives

$$\frac{\partial}{\partial t}\left[\frac{\partial^2 A}{\partial z^2} - k^2 A\right] = k(U-c)\left(Bk^2 - \frac{\partial^2 B}{\partial z^2}\right) + Bk\frac{\partial^2 U}{\partial z^2} + \frac{\partial^2}{\partial z^2}\left[\nu\left(\frac{\partial^2 A}{\partial z^2} + Ak^2\right)\right] + \nu k^2\left[\frac{\partial^2 A}{\partial z^2} + Ak^2\right] . \tag{14}$$

The sine terms give

$$\frac{\partial}{\partial t}\left[\frac{\partial^2 B}{\partial z^2} - k^2 B\right] = - k(U-c)\left(Ak^2 - \frac{\partial^2 A}{\partial z^2}\right) - Ak\frac{\partial^2 U}{\partial z^2} + \frac{\partial^2}{\partial z^2}\left[\nu\left(\frac{\partial^2 B}{\partial z^2} + Bk^2\right)\right] + \nu k^2\left[\frac{\partial^2 B}{\partial z^2} + Bk^2\right] . \tag{15}$$

When (11) and (13) are inserted into (9) we obtain

$$\frac{k}{2} \frac{\partial}{\partial z} [A \frac{\partial^2 B}{\partial z^2} - B \frac{\partial^2 A}{\partial z^2}] = \frac{\partial^2}{\partial z^2} (K \frac{\partial U}{\partial z}) \ . \tag{16}$$

Equations (14) - (16) clearly represent a coupled, non-linear system, in that terms such as $B \frac{\partial^2 U}{\partial z^2}$ occur. This essentially precludes analytical solution to the full set of equations. Yefimov proceeded by first considering the functions involved to be independent of time, thus reducing the system to one of ordinary differential equations for the steady state behavior. Furthermore, in (14) - (15) he approximated the mean flow [our $U(z,t)$ term] by the undisturbed log profile, $(U_*/\kappa) \ln (z/z_o)$, thus arriving at a linear system. After solving this system, by what he terms a "matrix distillation" method, he then solved for the deviation from the log profile by direct integration of the steady-state counterpart of (16). As noted in the introduction, a major part of our investigation concerns the effect of these neglected non-linear terms. Also note, as we shall return to it later, that (16) can be integrated twice to give a simpler equation for $\frac{\partial U}{\partial z}$.

3. Boundary Conditions

Determination of the correct boundary conditions for (14) - (16), specifically at the lower boundary is not as straightforward as the derivation of the equations. Yefimov (1970) defined the boundary conditions on the free surface at the lower boundary to be

$$U(\eta,t) + u(x,\eta,t) = - akc \cos k(x-ct) \ , \tag{17}$$

$$w(x,\eta,t) = akc \sin k(x-ct) \ ,$$

where the height of the free surface is given by

$$\eta = a \cos k(x-ct) \ . \tag{18}$$

Here a is the wave amplitude and $c = (g/k)^{1/2}$. He then assumed that the values of U, u and w on the free surface can be adequately approximated by their values at $z = 0$, if η is small. With u and w replaced by their values in terms of (11) and (13), this reduced to

$$\frac{\partial A}{\partial z}(0,t) = -akc , \qquad A(0,t) = ac$$
$$\frac{\partial B}{\partial z}(0,t) = 0 , \qquad B(0,t) = 0 . \tag{19}$$

However, note that (17) can be rewritten

$$U(\eta,t) + u(x,\eta,t) = -kc\eta ,$$

hence, it seems more correct that $u(x,\eta,t)$ can be approximated by its value at $z = 0$ only if $U(\eta,t)$ can also be (which is what Yefimov did). However, the Taylor expansion for $U(\eta,t)$ is

$$U(\eta,t) = U(0,t) + \left(\frac{\partial U}{\partial z}\right)_o \eta . \tag{20}$$

Since, for the standard logarithmic profile, $\left(\frac{\partial U}{\partial z}\right)_o \cong \frac{1}{z}$, it is very possible that $u(x,\eta,t) \not\cong u(x,0,t)$. Note that a similar difficulty with $w(x,0,t)$ is not likely, since $U(\eta,t)$ does not appear in this condition.

Since our main intent is the investigation of the effect of the non-linear terms in (14)-(16), we shall use (19) as our boundary condition. However, since our results are at variance with the observational studies, further consideration of alternative formulations to (19) seems warranted.

Note, a consequence of Yefimov's boundary conditions is that, near $z = 0$,

$$A(z,t) = O(1) \quad \text{and} \quad B(z,t) = O(z^2) .$$

Then, if one assumes that $U(z,t)$ is also $O(1)$, as well as second order and higher derivatives of A and B, then (15) implies that

$$\frac{\partial^2 U}{\partial z^2} = O(1) \text{ , near } z = 0 \text{ .}$$

This apparently induced Yefimov to use $\frac{\partial^2 U}{\partial z^2} = 0$ at the lower boundary in his numerical scheme.

Because of the requirement that the perturbations die out at the upper boundary $(z = H)$, both $A(z,t)$ and $B(z,t)$, as well as their first derivatives are set to zero at $z = H$.

4. Representation of the Mean Wave Field

We remark that in the case of no wave (i.e., $a = 0$), the solution to (14) - (16), plus the boundary conditions, is the log profile

$$A(z,t) = B(z,t) = 0 \text{ ,}$$

$$U(z,t) = \frac{U_*}{\varkappa} \ln \left(\frac{z}{z_o} + 1\right) \text{ .}$$

Note, this representation for the log profile does not generate a singularity at $z = 0$. Also note, from (16), this immediately implies a form for the diffusion coefficient

$$K = \varkappa\, U_* \, (z + z_o) \text{ .} \qquad (21)$$

Now, in the general case $(a \neq 0)$, there will be a departure from the log profile which we represent

$$U(z,t) = \frac{U_*}{\varkappa} \ln \left(\frac{z}{z_o} + 1\right) + \tilde{u}(z,t) \text{ ,} \qquad (22)$$

where

U_* = friction velocity, z_o = surface roughness, κ= von Karmon's constant.

When (22) is substituted in equation (16), and the resulting relation integrated, we have

$$\tilde{u} = - \int_o^z \frac{1}{K} \tau_w \, dz \tag{23}$$

where the wave induced stress is

$$\tau_w = - \widetilde{uw} = - \frac{1}{2} k \left(\frac{\partial B}{\partial z} A - \frac{\partial A}{\partial z} B\right) . \tag{24}$$

We note that Yefimov (1970) replaced the diffusion coefficient K in (23) by a constant ν, which is apparently the eddy viscosity coefficient used in (6). Whether this was a misprint in the translation is not clear, and we investigated the solutions for both K as given by (21) and with $K = \nu$.

5. Numerical Solution Procedure

As noted above, Yefimov solved the linearized steady-state equivalents of (14) - (15) by a procedure described only by the term "matrix distillation." In contrast, we chose to solve the time-dependent non-linear system (14), (15), (22) - (24) by difference equations, and time iterate until a numerical steady state evolved. To implement this, (14) and (15) were first reduced to difference equation form, using central finite differences on all spatial operations and all time operations except the diffusion terms (i.e., those with coefficient ν). The latter were evaluated at the previous time step in order to eliminate a diffusive instability. The left hand sides of these equations were then solved for the true tendencies with the Gauss elimination technique described in Richtmyer (1957). Leapfrog time differencing was used except that the integration was restarted every 50 time steps with the finite difference scheme developed by Matsuno (1966). This procedure eliminates solution separation.

The values of $A(z,t)$ and $B(z,t)$ thus computed are used to update the mean wind, as given by (21) - (24), and this updated mean wind is then used to compute $A(z,t)$ and $B(z,t)$ at the next time step. The boundary conditions take the following finite difference form

$$A(0,t) = ac \,, \tag{25}$$

$$B(0,t) = 0 \,, \tag{26}$$

$$\frac{A(\Delta z,t) - A(0,t)}{\Delta z} = - akc \,, \tag{27}$$

$$\frac{B(\Delta z,t) - B(0,t)}{\Delta z} = 0 \,, \tag{28}$$

$$A(H,t) = B(H,t) = 0 \,, \tag{29}$$

$$\frac{A(H,t) - A(H-\Delta z,t)}{\Delta z} = \frac{B(H,t) - B(H-\Delta t)}{\Delta z} = 0 \,, \tag{30}$$

where Δz is the grid increment.

The following initial conditions were used to start the solution

$$A(z,0) = ac \sinh [k(H_1 - z)]/\sinh kH_1 \,, \tag{31}$$

$$B(z,0) = 0 \,,$$

$$U(z,0) = \frac{U_*}{\kappa} \ln \left(\frac{z}{z_o} + 1\right) \,, \tag{32}$$

where $H_1 = H - \Delta z$. Note, the fields (31) represent potential flow over the waves.

From these initial conditions, as noted above, the time integration of the system of equations is accomplished by first predicting A and B from

(14) and (15) and then by obtaining U from (21) - (24). The integration is continued until the quantity

$$S_\tau = \left[\sum_{i=1}^{\frac{H}{\Delta z} - 1} [\tau(z_i,t) - \tau(z_i,t - \Delta t)]^2 \right]^{1/2} , \tag{33}$$

satisfies the condition

$$S_\tau < 10^{-5} m^2 sec^{-1} . \tag{34}$$

Condition (34) is taken to describe steady state.

6. Observational studies

Our numerical results will be compared to the results of several observational studies which have considered this problem and have looked for a dependence on c/U_*. Brutsaert (1973) has suggested that the wind shear should have the following dependence

$$\frac{dU}{dz} = \frac{U_*}{\kappa z} [1 + \beta(\frac{c}{U_*} - \alpha)^2] , \tag{35}$$

for $c/U_* > \alpha$. From the data he found that

$$\beta = .006 \quad \text{and} \quad \alpha = 29 .$$

Davidson (1974) examined the wind at 10 meters with the BOMEX data and obtained the following relation

$$U_{10} = \frac{U_*}{.41} [\ln(\frac{z}{z_o}) + 6.57 \frac{Z}{L} + .16(\frac{c}{U_*} - 26.3)] . \tag{36}$$

These studies show increased wind due to the wave for $c/U_* > \alpha$ where α is between 25 and 30. We will see later that the assumption that $\tilde{u}$ is dependent on only c/U_* is probably too restrictive. In particular Brutsaert (1973) assumed that the wave stress is constant in height which is neither reasonable nor consistent with observations.

7. Numerical results

The numerical model, as described above, was integrated for a number of the waves considered by Yefimov (1970) and, as a test, the system was made linear by setting $\tilde{u}$ equal to zero. When the dimensions were restored to Yefimov's solution, the comparison was quite good. It should be noted here that Yefimov non-dimensionalized his variables by scaling, and the results he presented corresponded to unscaled values of U_* in the range $0.01\ \text{msec}^{-1} < U_* < 0.05\ \text{msec}^{-1}$, or approximately an order of magnitude smaller than the values for which Davidson and Brutsaert obtained experimental data. The results which will be shown use the following values for the various parameters, unless otherwise noted:

$$\begin{aligned}
\Delta Z &= 0.25\text{m} \\
\Delta t &= 0.0125\text{sec} \\
H_1 &= 20\text{m} \\
\kappa &= 0.35 \\
z_o &= 3 \times 10^{-4}\text{m} \\
a &= 0.1/k
\end{aligned} \tag{37}$$

The value for H_1 was selected after numerical experiments showed larger values did not significantly alter the wind field at the values of c and U_* of interest.

Fig. 1 shows a typical stress field prediction for the linear (Yefimov) model for different values of U_*, at wave number $k = 0.25\text{m}^{-1}$ and

$\nu = 0.24\ m^2 sec^{-1}$. The values for k and U_* are typical for the BOMEX data used by Davidson, and the value for ν is that used by Yefimov. All of the curves have the same general pattern, with initially growing amplitude with increasing U_*, up to some maximum amplitude, followed by decreasing amplitude for further increases in U_*. Yefimov referred to this as a resonance-like behavior.

Fig. 2 presents the stress field predicted for the same wave number and values of U_* using the full non-linear model. Observe the qualitative behaviors are similar; however, two important quantitative differences emerge. First, the magnitude of the maximum stress amplitude for the non-linear model is only about 35% of that predicted by the linear model. We found this pattern consistently through all ranges of wave numbers considered, with the maximum stress amplitude predicted by the non-linear model usually only one-quarter to one-half that of the linear model. Secondly, note the apparent "resonance" is noticeably less pronounced in the non-linear case. This pattern also appeared consistently over the range of wave numbers. From these observations, we have concluded that the presence of the non-linear terms in (14) - (16) acts strongly to damp the wave induced stresses, and that to approximate (14) - (16) linearly, as Yefimov did, is not valid. Some further calculations were carried out with $ak = .05$ rather than the value $ak = 0.1$ that was used by Yefimov. With this relation for a the comparison between the linear and nonlinear solutions was closer except for the longer waves near $k = .05\ m^{-1}$. As a final point, note that both models predict the main contributions to the stress field occur in the lowest 5-8 meters. This is especially important, since both experimental studies referred to above have limited or non-existent data in this region.

In comparing these figures to the wind shear hypothesized by Brutsaert, (35), it is obvious that neither the linear nor the non-linear models agree with his assumption of constant stress at all heights. As noted above, we feel this assumption was too restrictive, though until additional data is obtained in the region below 8 meters it cannot be fully discounted.

To compare the results of the numerical models with Davidson's, we examined the deviation from the logarithmic profile predicted by Davidson:

$$\tilde{u}_{10} = U_{10} - \frac{U_*}{0.41} \ln \left(\frac{10}{z_o}\right) = \frac{0.16}{0.41} (c - 26.3\ U_*) \ , \qquad (38)$$

$$c > 27.5\ U_*$$

for the neutral case, with our predicted steady state value of $\tilde{u}(10,t)$, over a range of representative values of c and U_*. Fig. 3 shows the level curves of $\tilde{u}_{10}$ predicted by Davidson. Note that, even allowing for uncertainties in the determination of numerical coefficients, Davidson predicts essentially linear isolines. Fig. 4 shows the isolines determined by our non-linear model, using (21) to determine the diffusion coefficient, K. Although there are obviously regions, especially near the line $c = 27.5\ U_*$, where locally linear isolines occur, it is clear that our model will not produce this behavior globally. More seriously, although generally our model predicts increasing magnitude for the deviation as (c/U_*) increases, which is consistent with Davidson's observations, the algebraic sign is not consistent for observations show a positive deviation growing in magnitude, while our model predicts a negative deviation growing in magnitude.

The observed sign of $\tilde{u}$ at 10 meters could be obtained by reversing the curves in Fig. 2 or by distorting them in such a way that the negative area would be larger than the positive area. Davidson (1974) did observe negative stresses at the 3 meter level and in an earlier study with Lake Michigan data Davidson and Frank (1973) found positive stresses in the lower layers. It is not clear at present how our model could be restructured to reverse this algebraic sign, although we suspect that the boundary conditions are the major influence. There are two specific areas of the boundary conditions that we feel need more study. The first of these is the adequacy of replacing values for the horizontal components on the free surface by their values on the mean surface, as was discussed in section 3. A second point is the validity of the parameterization of the turbulent stresses used by Yefimov (see Eqs. (6) and (7)). The behavior of these stresses near the water surface is particularly crucial.

Figs. 5, 6, and 7 show the isolines predicted by other variants on the model. Those in Fig. 5 are derived from the linear model. Those in Fig. 6 are obtained from our non-linear model, by replacing the variable diffusion coefficient, K in (23), by the constant ν, as Yefimov's paper indicated. The curves in Fig. 7 are derived using a ν which varied with U_* according to

$$\nu = 1.2 \sec^{-1} U_* . \qquad (39)$$

This was suggested by the development of Davis (1974). Except for the linear model's unacceptably large predictions for the deviation (due to the "damping" we hypothesized in the non-linear model), all of these share the same qualitative features as we discussed for Fig. 4. This essentially leads us to believe, as mentioned above, that any changes in algebraic sign of the deviations must be through changes in the boundary conditions, or perhaps through the formulation of the wave induced turbulent diffusion.

8. Conclusions

The purpose of this paper was to investigate the linear model proposed by Yefimov from two aspects. First, to determine the effect of the non-linear terms neglected by him, and secondly to determine the agreement between predictions by the linear and non-linear models and observational studies by Davidson (1974) and Brutsaert (1973), which appeared after Yefimov's work.

The main conclusions of this study are that the non-linear terms neglected by Yefimov are in fact quite important when $ak = 0.1$, and impart a strong damping to the induced fields, that neither a linear nor a non-linear model will produce a height-independent stress as predicted by Brutsaert, and that although the non-linear model produces some agreement with Davidson's observations, there are also important disagreements, the most important being in algebraic sign. However, since the model predicts the major contribution to the induced stress to occur in the region near the mean surface, and since there are significant questions about the proper type of the mathematical boundary conditions, resolution of the differences and determination of how the model should be modified to produce results more consistent with observation demands more complete observational data on the induced stresses near the surface.

Acknowledgments: This research was supported by the Ocean Science Division of the Office of Naval Research in Arlington, Virginia. A. L. Schoenstadt was also supported by the Foundation Research Program of the Naval Postgraduate School which is funded by the Chief of Naval Research. The manuscript was carefully typed by Ms. M. Marks and the figures were drafted by Mr. P. Adler. The numerical computations were performed by the W. R. Church Computer Center.

References

Brutsaert, W., 1973: Similarity functions for turbulence in neutral air above swell. J. Phys. Oceanogr., 3, 479-482.

Davidson, K. L., 1974: Observational results on the influence of stability and wind-wave coupling on momentum transfer and turbulent fluctuations over ocean waves. Boundary-Layer Meteorology, 6, 305-331.

_____, and A. J. Frank, 1973: Wave-related fluctuations in the airflow over natural waves. J. Phys. Oceanogr., 3, 102-119.

Davis, R. E., 1970: On the turbulent flow over a wavy boundary. J. Fluid Mech., 42, 721-731.

_____, 1972: On prediction of the turbulent flow over a wavy boundary. J. Fluid Mech., 52, 287-306.

_____, 1974: Perturbed turbulent flow, eddy viscosity and the generation of turbulent stresses. J. Fluid Mech., 63, 673-693.

Lee, F. A., 1972: Some nonlinear aspects of wind-generated waves. J. Phys. Oceanogr., 2, 432-438.

Matsuno, T., 1966: Numerical integrations of the primitive equations by a simulated backward difference method. J. Meteorol. Soc. Japan, 44, 76-84.

Miles, J. W., 1957: On the generation of surface waves by shear flows. J. Fluid Mech., 3, 185-204.

Phillips, O. M., 1957: On the generation of waves by the turbulent wind. J. Fluid Mech., 2, 417-445.

Reynolds, W. C. and A.K.M.F. Hussain, 1972: The mechanics of an organized wave in turbulent shear flow. Part 3: Theoretical models and comparisons with experiments. J. Fluid Mech., 54, 263-288.

Richtmyer, R. D., 1957: Difference Methods for Initial Value Problems. Interscience Publishers, Inc., New York, 238 pp.

Yefimov, V. V., 1970: On the structure of the wind velocity field in the atmospheric near-water layer and the transfer of wind energy to sea waves. Izv., Atmospheric and Oceanic Physics, 6, 1043-1058, translated by J. D. L. McIntosh.

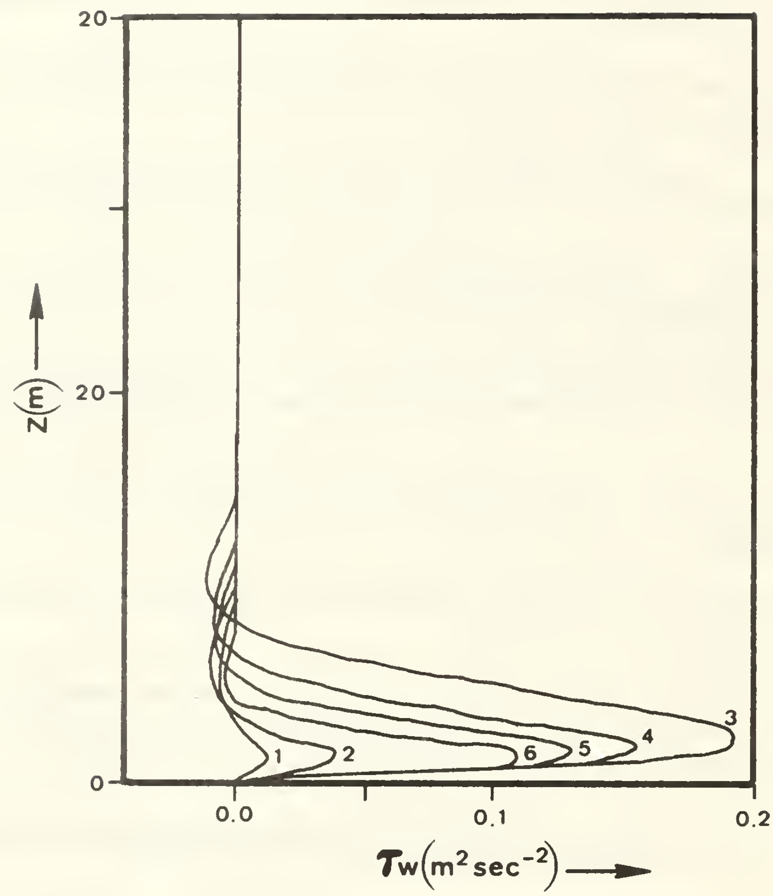

FIGURE 1

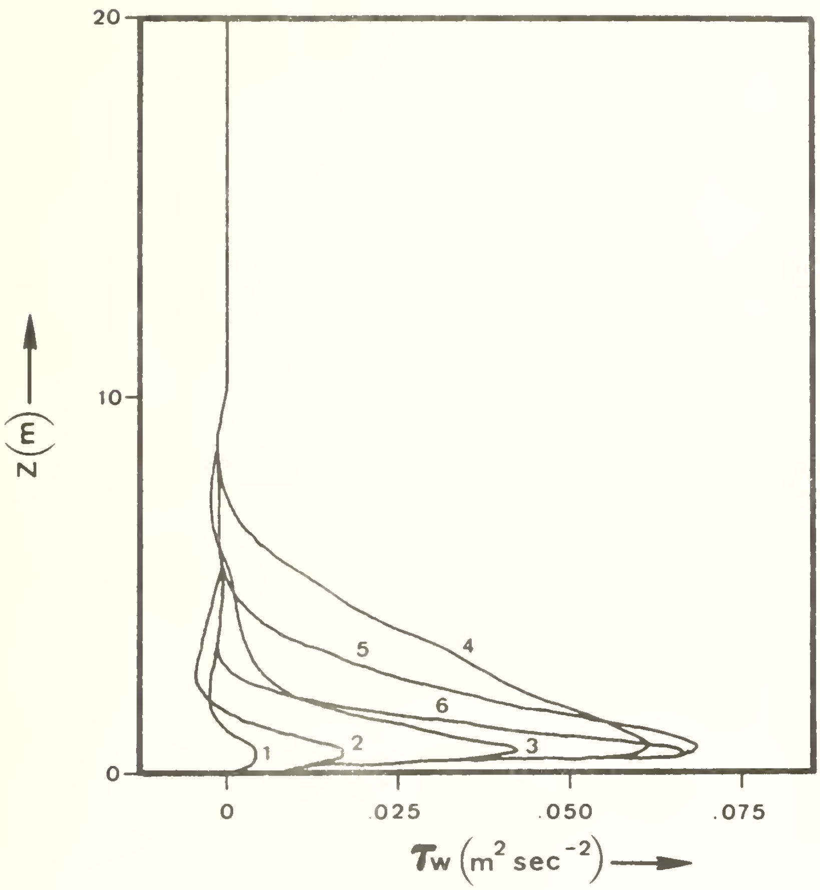

FIGURE 2

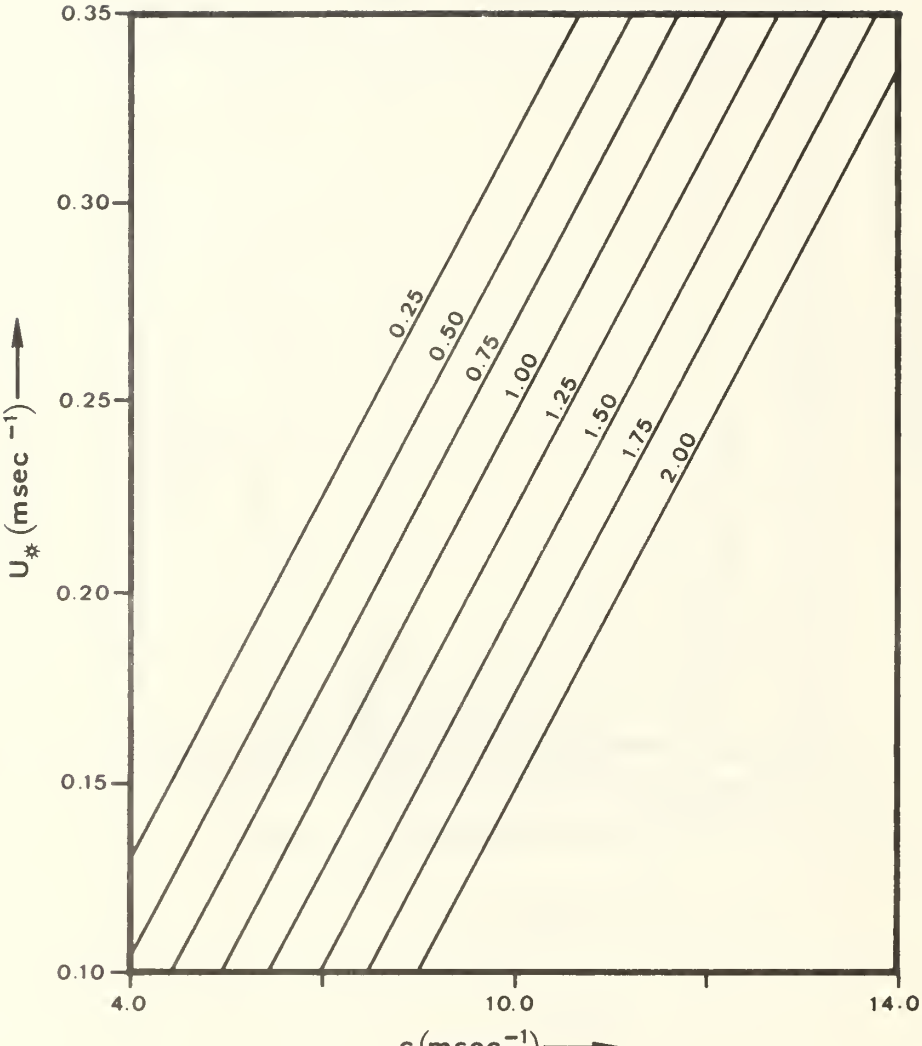
0.35
0.30
0.25
0.20
0.15
0.10
4.0
10.0
14.0
U* (msec⁻¹)
c (msec⁻¹)
0.25
0.50
0.75
1.00
1.25
1.50
1.75
2.00

FIGURE 3

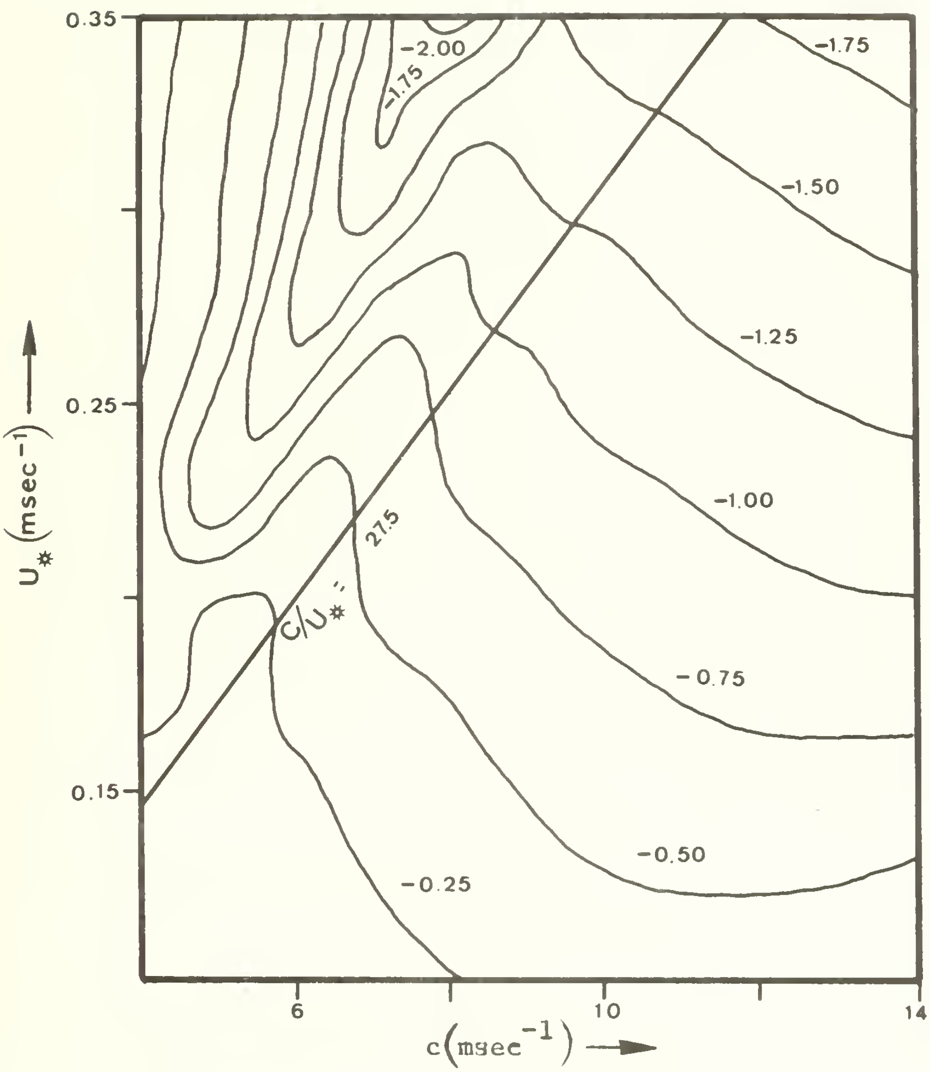

0.35
0.25
0.15
$u_*\,(\mathrm{msec}^{-1})$
6
10
14
$c\,(\mathrm{msec}^{-1})$
−2.00
−1.75
−1.75
−1.50
−1.25
−1.00
− 0.75
−0.50
−0.25
$c/u_* = 27.5$

FIGURE 4

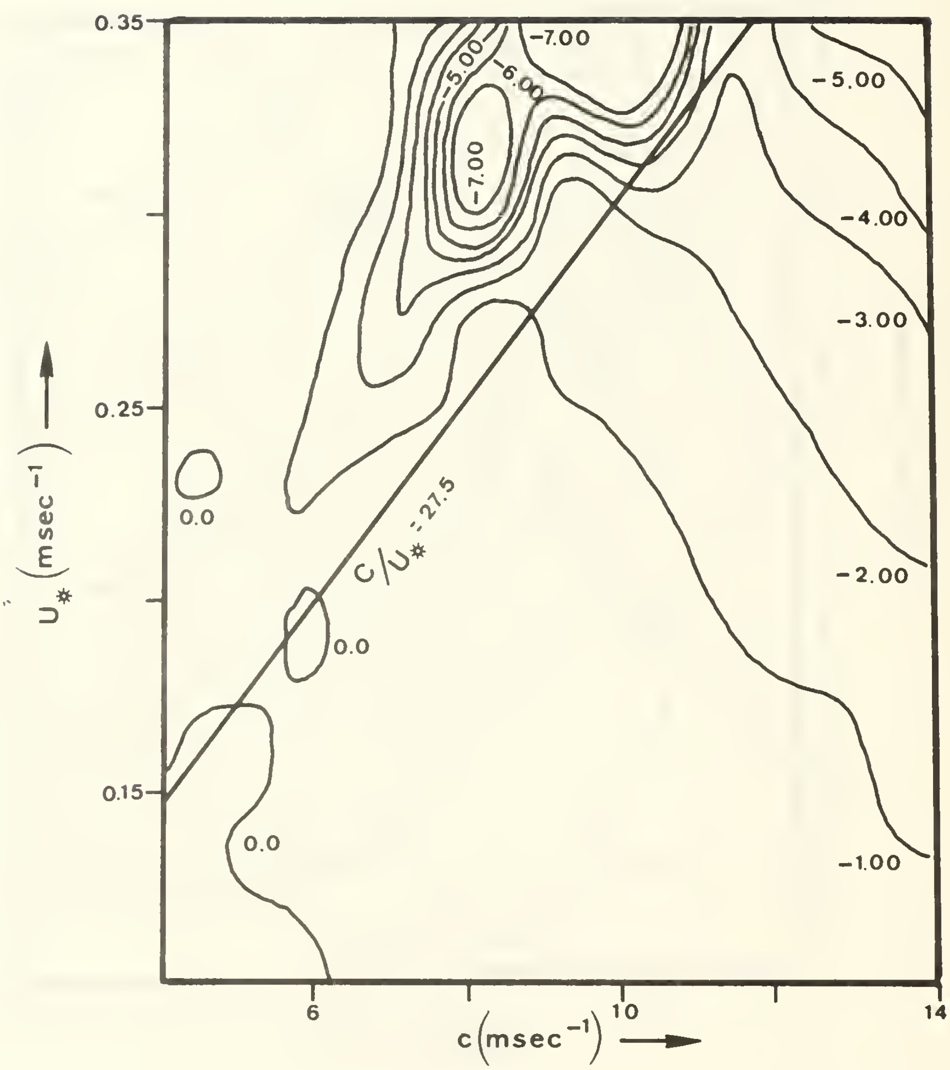

0.35
0.25
0.15
-7.00
-5.00
-6.00
-7.00
-5.00
-4.00
-3.00
-2.00
-1.00
0.0
0.0
0.0
c/U* = 27.5
6
10
14
U_*' (msec^{-1})
c (msec^{-1})

FIGURE 5

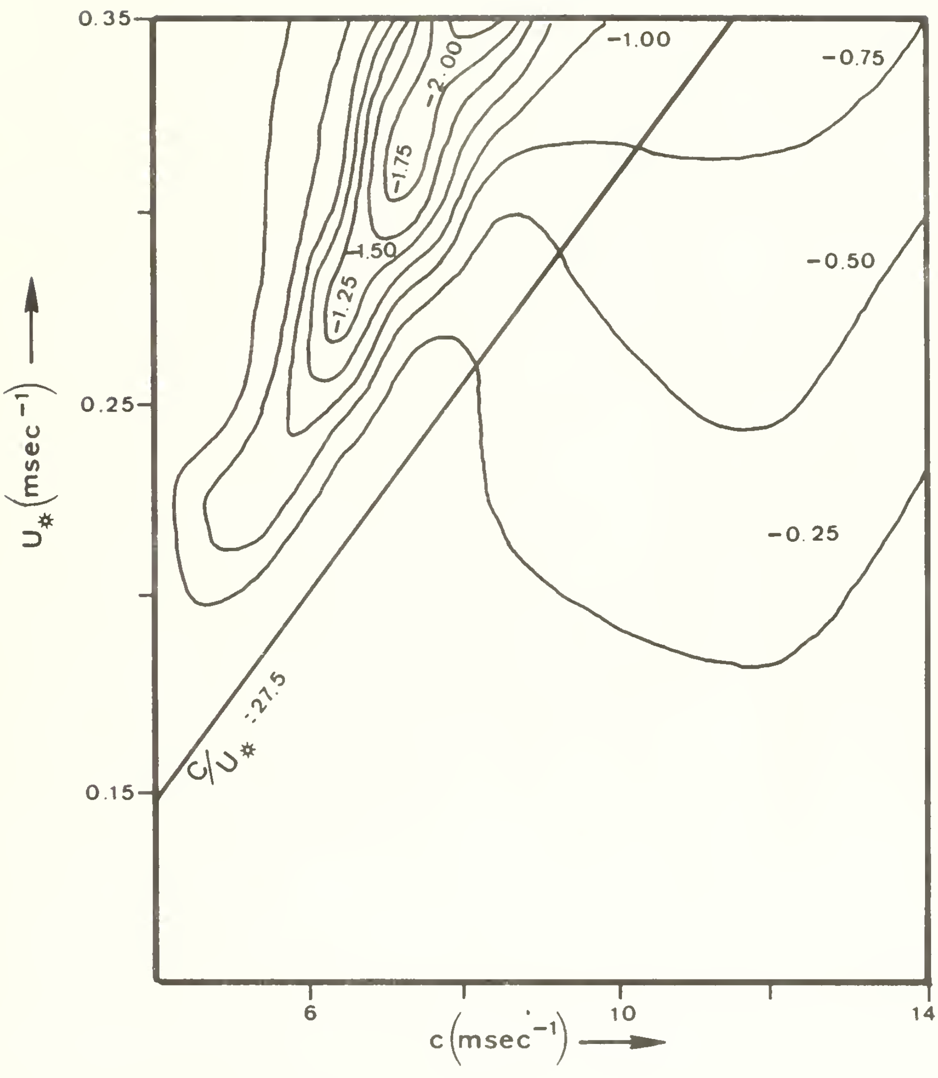

0.35
0.25
0.15
6
10
14
c (msec⁻¹)
U* (msec⁻¹)
-1.00
-0.75
-0.50
-0.25
-2.00
-1.75
-1.50
-1.25
C/U* = 27.5

FIGURE 6

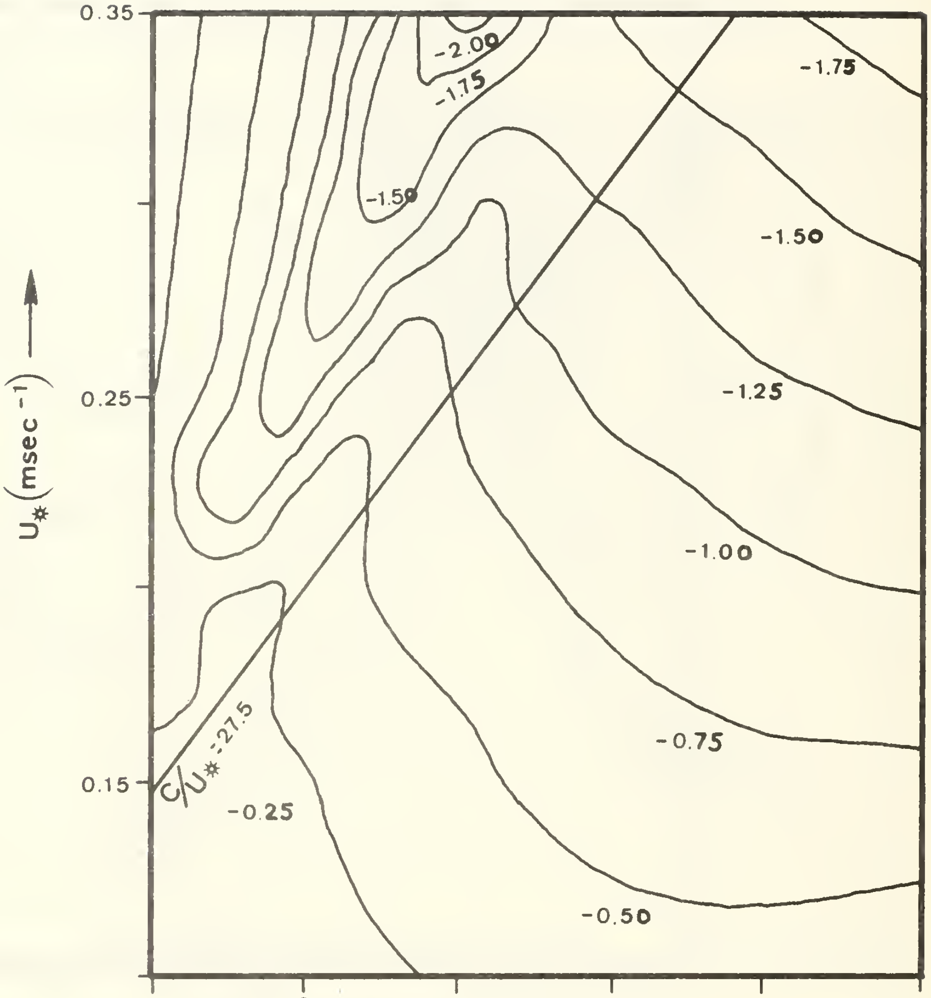
0.35
0.25
0.15
6
10
14
c (msec⁻¹)
U* (msec⁻¹)
-2.00
-1.75
-1.50
-1.75
-1.50
-1.25
-1.00
-0.75
-0.50
-0.25
C/U* = 27.5

FIGURE 7

DISTRIBUTION LIST

		No. Copies
1.	Defense Documentation Center Cameron Station Alexandria, Virginia 22314	12
2.	Library, Code 0212 Naval Postgraduate School Monterey, California 93940	2
3.	Dr. R. T. Williams, Code 51Wu Department of Meteorology Naval Postgraduate School Monterey, California 93940	10
4.	Dr. A. L. Schoenstadt, Code 53Zh Department of Mathematics Naval Postgraduate School Monterey, California 93940	10
5.	Chief of Naval Research Attn: Ocean Science Division Arlington, Virginia 22217	2
6.	Dr. K. L. Davidson, Code 51Ds Department of Meteorology Naval Postgraduate School Monterey, California 93940	10
7.	Commanding Officer Naval Weather Service Command Headquarters 3101 Building 200 Washington Navy Yard Washington, D. C. 20374	1
8.	Officer in Charge Environmental Prediction Research Facility Naval Postgraduate School Monterey, California 93940	2
9.	Dean of Research Naval Postgraduate School Monterey, California 93940	2
10.	Commanding Officer Fleet Numerical Weather Central Naval Postgraduate School Monterey, California 93940	2

11. Naval Oceanographic Office 1
Library (Code 3330)
Washington, D. C. 20373

12. AFCRL - Research Library 1
L. G. Hanscom Field
Attn: Nancy Davis/Stop 29
Bedford, Massachusetts 01730

13. Commander, Air Weather Service 1
Military Airlift Command
United States Air Force
Scott Air Force Base, Illinois 62226

14. Dr. R. Alexander 1
The RAND Corporation
1700 Main Street
Santa Monica, California 90406

15. Dr. A. Arakawa 1
Department of Meteorology
University of California
Los Angeles, California 90024

16. Atmospheric Sciences Library 1
National Oceanic and Atmospheric Administration
Silver Spring, Maryland 20910

17. Dr. Wilfred Brutsaert 1
Cornell University
Ithaca, New York 14850

18. Dr. C. P. Chang, Code 51Cj 1
Department of Meteorology
Naval Postgraduate School
Monterey, California 93940

19. Professor J. G. Charney 1
54-1424
Massachusetts Institute of Technology
Cambridge, Massachusetts 02139

20. Dr. Russ Davis 1
University of California at San Diego
San Diego, California 92037

21. LT K. G. Dunning 1
USS Agerholm
FPO, San Francisco, California 96601

22. Dr. R. L. Elsberry, Code 51Es 1
Department of Meteorology
Naval Postgraduate School
Monterey, California 93940

23. Dr. John C. Freeman 1
Institute for Storm Research
3812 Montrose Blvd.
Houston, Texas 77006

24. Dr. J. A. Galt 1
NOAA - Pac. Mar. Envir. Lab.
University of Washington WB-10
Seattle, Washington 98105

25. Dr. W. L. Gates 1
The RAND Corporation
1700 Main Street
Santa Monica, California 90406

26. Dr. Earl Gossard 1
Wave Propagation Laboratory
NOAA/ERL
Boulder, Colorado 80302

27. Dr. T. Green 1
Department of Meteorology
University of Wisconsin
Madison, Wisconsin 53706

28. Dr. G. J. Haltiner, Code 51Ha 1
Chairman, Department of Meteorology
Naval Postgraduate School
Monterey, California 93940

29. Dr. R. L. Haney, Code 51Hy 1
Department of Meteorology
Naval Postgraduate School
Monterey, California 93940

30. Dr. J. Holton 1
Department of Atmospheric Sciences
University of Washington
Seattle, Washington 98105

31. Dr. Joseph Huang 1
Great Lake Environmental Res. Lab.
NOAA
2300 Washtenaw Avenue
Ann Arbor, Michigan 48104

32. Dr. S. K. Kao 1
Department of Meteorology
University of Utah
Salt Lake City, Utah 84112

33. Dr. B. Katz, Code 432 3
Naval Surface Weapons Center
White Oak
Silver Springs, Maryland 20910

34. Dr. Ladis D. Kovach, Code 53Kv 1
Chairman, Department of Mathematics
Naval Postgraduate School
Monterey, California 93940

35. Dr. C. E. Leith 1
National Center for Atmospheric Research
P. O. Box 3000
Boulder, Colorado 80303

36. Dr. J. M. Lewis 1
Laboratory for Atmospheric Research
University of Illinois
Urbana, Illinois 61801

37. Dr. E. N. Lorenz 1
Department of Meteorology
Massachusetts Institute of Technology
Cambridge, Massachusetts 02139

38. Dr. J. D. Mahlman 1
Geophysical Fluid Dynamics Laboratory
Princeton University
Princeton, New Jersey 08540

39. Meteorology Library (Code 51) 1
Naval Postgraduate School
Monterey, California 93940

40. National Center for Atmospheric Research 1
Box 1470
Boulder, Colorado 80302

41. Director, Naval Research Laboratory 1
Attn: Technical Services Information Center
Washington, D. C. 20390

42. Dr. E. C. Nickerson 1
NOAA
Atmospheric Physics and Chemistry Laboratory
Boulder, Colorado 80302

43. Department of Oceanography, Code 58 1
Naval Postgraduate School
Monterey, California 93940

44. Dr. J. J. O'Brien, Code 481 2
Office of Naval Research
Arlongton, Virginia 22217

45. Office of Naval Research 1
Department of the Navy
Washington, D. C. 20360

46. Professor N. A. Phillips 1
National Meteorological Center/NOAA
World Weather Building
Washington, D. C. 20233

47. Dr. S. Piacsek 1
Code 7750
Naval Research Laboratory
Washington, D. C. 20390

48. Dr. Hillel Rubin 1
Civil Engineering Department
University of Florida
Gainesville, Florida 32611

49. Dr. Joanne Simpson 1
Department of Environmental Sciences
2015 Ivy Road
Charlottesville, Virginia 22903

50. Dr. J. Smagorinsky, Director 1
Geophysical Fluid Dynamics Laboratory
Princeton University
Princeton, New Jersey 08540

51. Professor B. Lincoln Smith 2
Department of Marine Sciences
Center for Wetland Resources
Louisiana State University
Baton Rouge, Louisiana 70803

52. LCDR B. C. Stauffer 1
Fleet Numerical Weather Central
Monterey, California 93940

53. Dr. M. G. Wurtele 1
Department of Meteorology
University of California
Los Angeles, California 90024

54. Dr. J. Young 1
Department of Meteorology
University of Wisconsin
Madison, Wisconsin 53706